JVI Journals.ASM.org

Increased Interaction between Vaccinia Virus Proteins A33 and B5 Is Detrimental to Infectious Extracellular Enveloped Virion Production

Winnie M. Chan* and Brian M. Ward

Department of Microbiology and Immunology, University of Rochester Medical Center, Rochester, New York, USA

Two mechanisms exist for the incorporation of B5 into extracellular virions, one of which is dependent on A33. In the companion to this paper (W. M. Chan and B. M. Ward, J. Virol. 86:8210–8220, 2012), we show that the lumenal domain of A33 is sufficient for interaction with the coiled-coil domain of B5 and capable of directing B5-green fluorescent protein (GFP) into extracellular virions. Here, we have created a panel of charge-to-alanine mutations in the lumenal domain of A33 to map the B5 interaction site. While none of these mutations abolished the interaction with B5, a subset displayed an increased interaction with both B5 and B5-GFP. Both B5 and B5-GFP recombinant viruses expressing these mutant proteins in place of normal A33 had a small-plaque phenotype. The increased interaction of the mutant proteins was detected during infection, suggesting that normally the interaction is either weak or transient. In addition, the increased A33-B5 interaction was detected on virions produced by recombinant viruses and correlated with reduced target cell binding. Taken together, these results show that both B5 and B5-GFP interact with A33 during infection and that the duration of this interaction needs to be regulated for the production of fully infectious extracellular virions.

Vaccinia virus, the prototypical member of the family *Poxviridae*, was used as a live-attenuated vaccine for the eradication of smallpox. It is a double-stranded DNA virus with a genome of about 200 kbp that is predicted to encode approximately 200 functional open reading frames (22). Replication in the cytoplasm results in two infectious forms, intracellular mature viruses (IMV) and extracellular viruses (EV) (7, 28). EV arise from IMV that have been wrapped in additional membranes derived from the *trans*-Golgi complex or early endosome (16, 32, 36) and are actively released from infected cells to spread infection. The process of wrapping IMV to form EV produces intermediate forms called intracellular enveloped virions (IEV) that contains two more membranes than IMV and one less membrane than the released EV form. The vaccinia virus proteins A33 (29), A34 (8), A56 (33), B5 (11, 47), F13 (1), and K2 (37, 40) are found on both the IEV and EV forms, whereas F12 (38, 50) and A36 (39) are found only on the IEV form. Deletion of any of the genes corresponding to these proteins, except for A56R and K2L, results in a small-plaque phenotype, indicating that they are involved in IEV formation, egress, and/or infectivity of EV.

Multiple interactions between the EV and IEV proteins have been demonstrated. The B5 protein has been reported to interact with A33, A34, and F13 (3, 5, 6, 10, 24–26, 31). B5R encodes a 42-kDa type I glycoprotein that is involved in EV formation (11, 12, 18, 47). The lumenal domain of B5 contains four short consensus repeats (SCRs), which represent most of the extracellular domain, followed by a predicted coiled-coil domain that precedes the transmembrane domain and a short cytoplasmic tail (11, 18). The coiled-coil domain is sufficient for interaction with the lumenal domain of A33 (4), while deletion of either the cytoplasmic tail or the four SCRs of B5 does not affect EV formation (15, 21).

A33R is predicted to encode a 21-kDa type II glycoprotein (29) with a predicted C-type lectin-like domain (35). It has been shown to form homodimers that can be linked by interprotein disulfide bonds (3, 30). A33 has been shown to be required for efficient target cell binding by EV, and deletion of A33R results in the release of more EV from the cell surface with reduced infectivity (5, 30). During morphogenesis, A33 interacts with IEV protein A36 through the cytoplasmic tail (46, 49). The interaction is required for the incorporation of A36 into the outer envelope of IEV and, subsequently, virus-induced actin tail formation (48). A33 and B5/B5-green fluorescent protein (GFP) have been shown to interact during infection, as well as in the absence of vaccinia viral late proteins (3, 4, 25). In our companion paper, we report that the lumenal domain of A33 is sufficient for interaction with B5 while a transmembrane domain is required for the lumenal domain of B5 to interact with A33 (4). In addition, the interaction between the lumenal domains of A33 and B5 is required for the efficient incorporation of B5-GFP into EV (4). In this study, we created a set of mutations in A33 in an effort to map the B5 interaction domain. Our efforts led to the creation of a group of A33 charge-to-alanine (CTA) mutant proteins that had a more durable interaction with B5. Interestingly, we have found that the increased interaction between A33 and B5 is detrimental to the infectivity of EV. In addition, the presence of the A33-B5 complex on the surface of extracellular enveloped virions (EEV) reduces the ability of EEV to bind target cells, suggesting that the A33-B5 interaction must be transient for the production of fully infectious EEV.

MATERIALS AND METHODS

Cells. HeLa, BSC-1, and RK_{13} cells were maintained as previously described (42).

Plasmid constructs. The construction of pBMW118 (42), pA33R-HA, and pA33R full (3) has been described previously. To construct the

Received 30 January 2012 Accepted 14 May 2012

Published ahead of print 23 May 2012

Address correspondence to Brian M. Ward, Brian_Ward@urmc.rochester.edu.

* Present address: Department of Molecular Genetics and Microbiology, University of Florida, Gainesville, Florida, USA.

doi:10.1128/JVI.00253-12

CTA mutant proteins pA33R-HA$^{E67\text{-}D72}$, pA33R-HA$^{H84\text{-}K86}$, pA33R-HA$^{D95\text{-}E98}$, pA33R-HA$^{H113\text{-}K123}$, pA33R-HA$^{D138\text{-}D150}$, and pA33R-HA$^{D155\text{-}D170}$, forward and reverse primers containing the desired mutations were designed and two-step overlapping PCR was performed using pA33R-HA as the template. To construct pA33R-HA$^{E174\text{-}K182}$, a reverse primer containing the desired mutations and the coding sequence of a hemagglutinin (HA) epitope tag was designed. PCR products were inserted into pCR2.1 (Invitrogen) and subcloned into pcDNA3 (Invitrogen) to place the coding sequence under the control of the T7 promoter, as described previously (3). To generate recombinant viruses expressing the CTA mutant proteins in place of normal A33, two-step overlapping PCR was performed as described above, except that pA33R-full (3), a plasmid that contains the coding sequence of A33R flanked by ~500 bp of the upstream sequence, which contains the A33R promoter, and the downstream sequence, was used as the template. PCR products were inserted into pCR2.1 (Invitrogen) and subcloned into the multiple cloning site of *trans*-dominant selection vector pBMW118 (42) that had been digested with SalI and SmaI to yield pA33R$^{H84\text{-}K86}$-full, pA33R$^{D95\text{-}E98}$-full, pA33R$^{H113\text{-}K123}$-full, pA33R$^{D138\text{-}D150}$-full, pA33R$^{D155\text{-}D170}$-full, and pA33R$^{E174\text{-}K182}$-full. All constructs were verified by sequencing.

Construction of recombinant viruses. The construction of vB5R-GFP (45), vB5R-GFP/ΔA33R (5), and vTF7.3 (14) has been described previously. To construct recombinant viruses expressing an A33R-containing CTA mutation, HeLa cells were infected with vB5R-GFP/ΔA33R or vB5R-GFP at a multiplicity of infection (MOI) of 5.0 and transfected with pA33R$^{H84\text{-}K86}$-full, pA33R$^{D95\text{-}E98}$-full, pA33R$^{H113\text{-}K123}$-full, pA33R$^{D138\text{-}D150}$-full, pA33R$^{D155\text{-}D170}$-full, or pA33R$^{E174\text{-}K182}$-full. To generate vA33R$^{D95\text{-}E98}$/B5R and vA33R$^{E174\text{-}K182}$/B5R, HeLa cells were infected with either vΔA33R or WR and transfected with pA33R$^{D95\text{-}E98}$-full or pA33R$^{E174\text{-}K182}$-full, respectively. The next day, cells were scraped into medium and cell lysates were prepared by repeated freezing and thawing. Plasmid pBMW118 contains the coding sequences for HcRed and guanine phosphoribosyltransferase under the control of viral promoters. A previously described procedure for *trans*-dominant selection was used to select for single-crossover recombinants that expressed HcRed and were resistant to xanthine-guanine phosphoribosyltransferase selection (9, 42). Single-crossover recombinants were further plaque purified four times in the absence of a selection drug to obtain the desired double-crossover recombinant. To construct vA33R$^{E174\text{-}K182}$/ΔB5R, the gene for B5R in vA33R$^{E174\text{-}K182}$ was replaced with the coding sequence of mOrange (Clontech) that is under the control of the promoter of the gene for B5R. HeLa cells were infected with vA33R$^{E174\text{-}K182}$ and transfected with the PCR product of the mOrange (Clontech) coding sequence flanked by the B5R 500-bp upstream, containing the promoter sequence, and downstream regions. The next day, cells were harvested and cell lysates were plated on fresh BSC-1 cell monolayers. Plaques that fluoresced orange were picked and purified three more times. All of the recombinant viruses were amplified as described previously (9). The coding sequence of A33R from the recombinants was verified by sequencing.

Plaque assay. The procedure for the plaque assay used has been described previously (42). Briefly, confluent BSC-1 cell monolayers were infected with the indicated viruses. At 2 h postinfection (p.i.), the inoculum was removed and cell monolayers were overlaid with semisolid medium. At 3 days p.i., cell monolayers were stained with crystal violet and imaged.

Immunofluorescence microscopy. HeLa cells grown on glass coverslips were infected with recombinant viruses at an MOI of 1.0. The next day, cells were fixed with 4% paraformaldehyde in phosphate-buffered saline (PBS). For surface staining, fixed cells were incubated with either rabbit anti-A33 antiserum (BEI Resources) or an anti-B5 monoclonal antibody (MAb) 19C2 (32), followed by Texas Red-conjugated donkey anti-rabbit or anti-rat antibody (Jackson ImmunoResearch Laboratories), respectively. For intracellular staining, fixed cells were permeabilized with 0.1% Triton X-100 in PBS and stained with rabbit anti-A33 antiserum (BEI Resources) as described above. To visualize filamentous actin, immunostained cells were permeabilized and stained with Alexa Fluor 350-conjugated phalloidin (Invitrogen) by following the manufacturer's instructions. Images were minimally processed and pseudocolored using Adobe Photoshop software (Adobe Systems).

Immunoprecipitation and Western blotting. HeLa cells infected with vTF7.3 (14) at an MOI of 5.0 in the presence of 40 μg/ml of cytosine arabinoside (AraC) (Sigma) were transfected with various plasmids containing the coding sequences of genes under the control of the vaccinia virus T7 promoter at 2 h p.i. For radiolabeled immunoprecipitation, transfection medium was removed at 4 h posttransfection and replaced with medium containing 25 μCi/ml of [^{35}S]Met-Cys (Perkin-Elmer). The following day, cells were harvested by scraping, washed once in PBS, and lysed in radioimmunoprecipitation assay (RIPA) buffer (0.5× PBS, 0.1% sodium dodecyl sulfate, 1% Triton X-100, 1% NP-40, 0.5% sodium deoxycholate) containing protease inhibitors as previously described (5). Immunoprecipitation was performed using an anti-HA MAb (Santa Cruz Biotechnology) as previously described (10). Proteins were resolved on 4 to 12% Bis-Tris gradient gels (Invitrogen) and visualized by autoradiography. To verify the expression of constructs, cell lysates were resolved on 4 to 12% Bis-Tris gradient gels (Invitrogen). Proteins were transferred to nitrocellulose membranes and detected as described in the figure legends using the following antibodies: horseradish peroxidase (HRP)-conjugated anti-GFP antibody (Rockland), HRP-conjugated anti-HA antibody (Roche), anti-GFP MAb (Covance), and anti-HA MAb (Roche). HRP- and Cy5-conjugated, anti-mouse, anti-rat, and anti-rabbit antibodies were purchased from Jackson ImmunoResearch Laboratories. HRP was detected using chemiluminescent reagents (Pierce) by following the manufacturer's instructions. The fluorescent and chemiluminescent signal was captured using a Kodak Image Station 4000mmPro (Carestream Health Inc.) outfitted with appropriate filter sets.

To test the interaction between A33 and B5/B5-GFP during infection, HeLa cells were infected with recombinant viruses at an MOI of 5.0. The next day, cells were harvested and lysed and immunoprecipitation was performed using rabbit anti-A33 antiserum (BEI Resources) as described above. Western blotting was performed on cell lysates and immunoprecipitated proteins using an anti-B5 MAb (19C2), followed by an HRP-conjugated donkey anti-rat antibody (Jackson ImmunoResearch Laboratories). The blot with the immunoprecipitated proteins was stripped and reprobed with a rabbit anti-A33 antiserum, followed by an HRP-conjugated donkey anti-rabbit antibody (Jackson ImmunoResearch Laboratories).

Analysis of EEV. RK_{13} cells were infected with recombinant viruses at an MOI of 10.0. At 4 h p.i., the medium was replaced with medium containing [^{35}S]Met-Cys (Perkin-Elmer). The next day, radiolabeled virions released into the medium were purified through a 36% sucrose cushion. The resulting viral pellets were lysed in EEV lysis buffer (1% Triton X-100, 0.5% NP-40, 25 mM Tris-HCl, pH 7.4, 1 mM EDTA, 100 mM NaCl, protease inhibitor cocktail [Roche]). EEV lysates were equilibrated by scintillation counting, and equal counts were subjected to immunoprecipitation with an anti-B5 MAb, an anti-F13 MAb kindly provided by Jay Hooper, or a rabbit anti-A33 antiserum (BEI Resources). Antibody-protein complexes were pulled down as described previously (10). Immunoprecipitated proteins were analyzed by SDS-PAGE and detected by autoradiography.

Binding assay. The binding assay has been described previously (5). Briefly, RK_{13} cells were infected with vB5R-GFP, vA33R$^{E174\text{-}K182}$, vΔB5R, or vA33R$^{E174\text{-}K182}$/ΔB5R at an MOI of 10.0. At 24 h p.i., culture supernatants were collected and centrifuged at low speed to remove cell debris. The genome copy in the supernatants was determined using real-time PCR as described previously (5). The same numbers of virions, as equilibrated by genome copies, were bound to HeLa cells. EEV bound to cells were visualized by immunostaining with an anti-F13 MAb, followed by Texas Red-conjugated donkey anti-mouse antibody (Jackson ImmunoResearch Laboratories). The binding ability of EEV was determined by

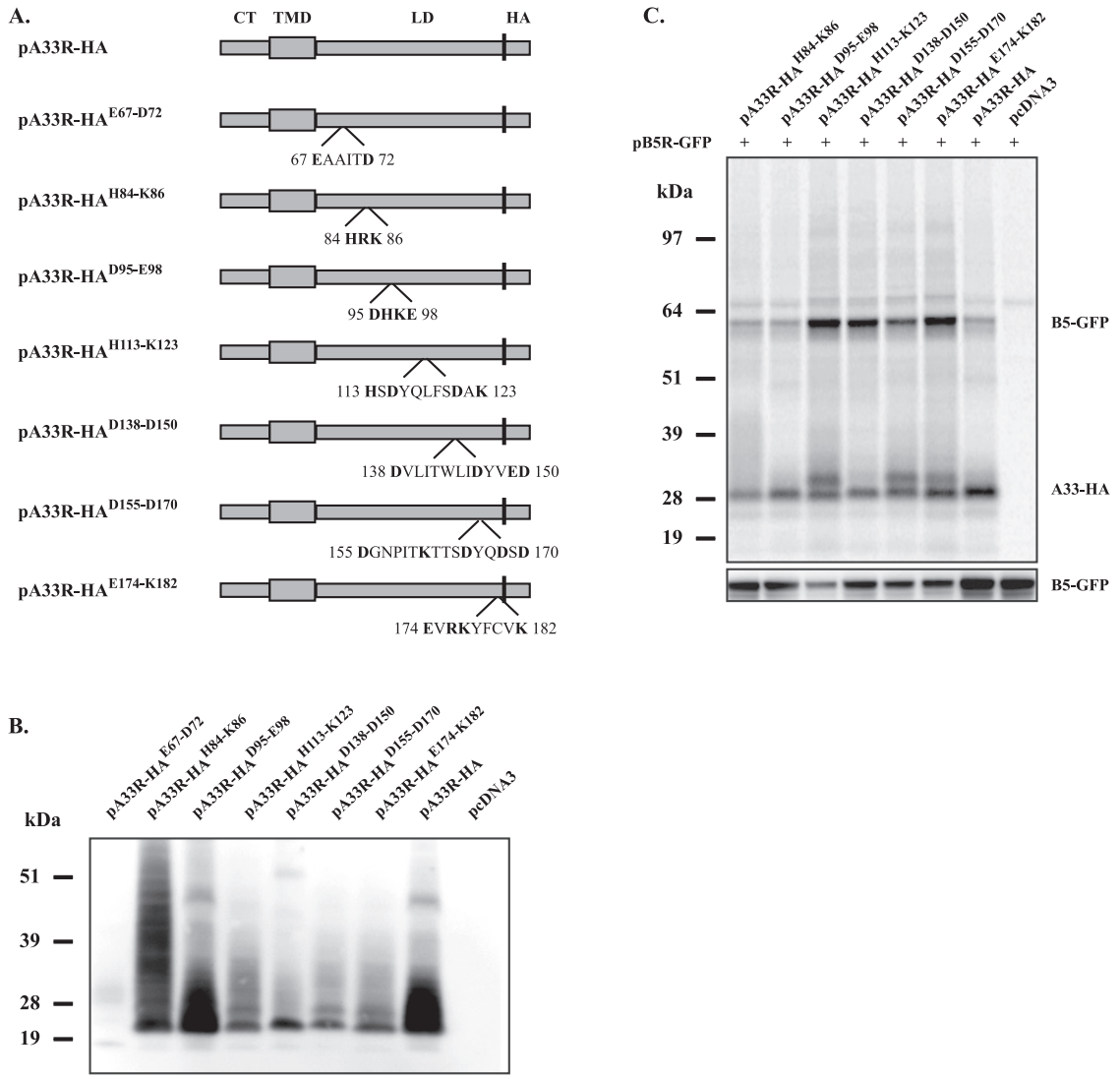

FIG 1 A33 CTA mutant proteins still interact with B5-GFP. (A) Diagrammatic representations of the positions of CTA mutations in A33-HA. The amino acid sequences of the mutated regions are shown with the charged residues mutated to alanine in bold. (B and C) Expression and CoIP of CTA mutant proteins. HeLa cells infected with vTF7.3 were transfected with the indicated plasmids in the presence of AraC. At 4 h posttransfection, the medium was replaced with medium containing [^{35}S]Met-Cys (C). At 24 h posttransfection, cells were harvested and lysed in RIPA buffer. Cell lysates were analyzed by Western blotting using an HRP-conjugated anti-HA antibody (B). Cell lysates were subjected to immunoprecipitation with an anti-HA antibody. Antibody-protein complexes were resolved by SDS-PAGE, and proteins were detected by autoradiography (C, top blot). Cell lysates were analyzed by Western blotting using an HRP-conjugated anti-GFP antibody (C, bottom blot) to examine the B5-GFP expression level. The molecular masses, in kilodaltons, and positions of marker proteins are shown on the left.

counting the F13-labeled virion-sized particles that were bound to 200 cells.

RESULTS

A33 CTA mutant proteins still interact with B5-GFP. A33 is a multifunctional protein, and we have found that the lumenal domain of A33 is sufficient for interaction with either B5 or B5-GFP (4). For B5-GFP, this interaction is required for its incorporation into EV. We wanted to map the specific residues in the lumenal domain of A33 that are involved in the B5 interaction. We therefore generated seven mutant forms of A33 that had clusters of charged residues mutated to alanine to test for interaction with B5-GFP (Fig. 1A). In addition, all of our constructs had the HA epitope tag appended to the C terminus. Initially, we checked the expression of our clustered CTA mutant proteins using the vaccinia virus T7 expression system in the presence of AraC, which blocks late viral protein synthesis. This system has several advantages, including high protein expression in the cytoplasm of the cell in the absence of other viral late proteins and therefore morphogenesis. To check expression, a Western blot assay of lysates from cells expressing the CTA mutant proteins was probed with an anti-HA MAb. With the exception of A33-HA$^{E67\text{-}D72}$, all of the constructs produced a smear between 25 and 30 kDa (Fig. 1B) that is typical of A33 and has been attributed to both N- and O-linked glycosylation (24, 29). The A33-HA$^{E67\text{-}D72}$ mutant protein was not included in the rest of our analysis due to the poor level of expression. We next tested for an interaction with B5-GFP. Each mutant protein was coexpressed with B5-GFP using the same T7 system and assessed for interaction by coimmunoprecipitation (CoIP)

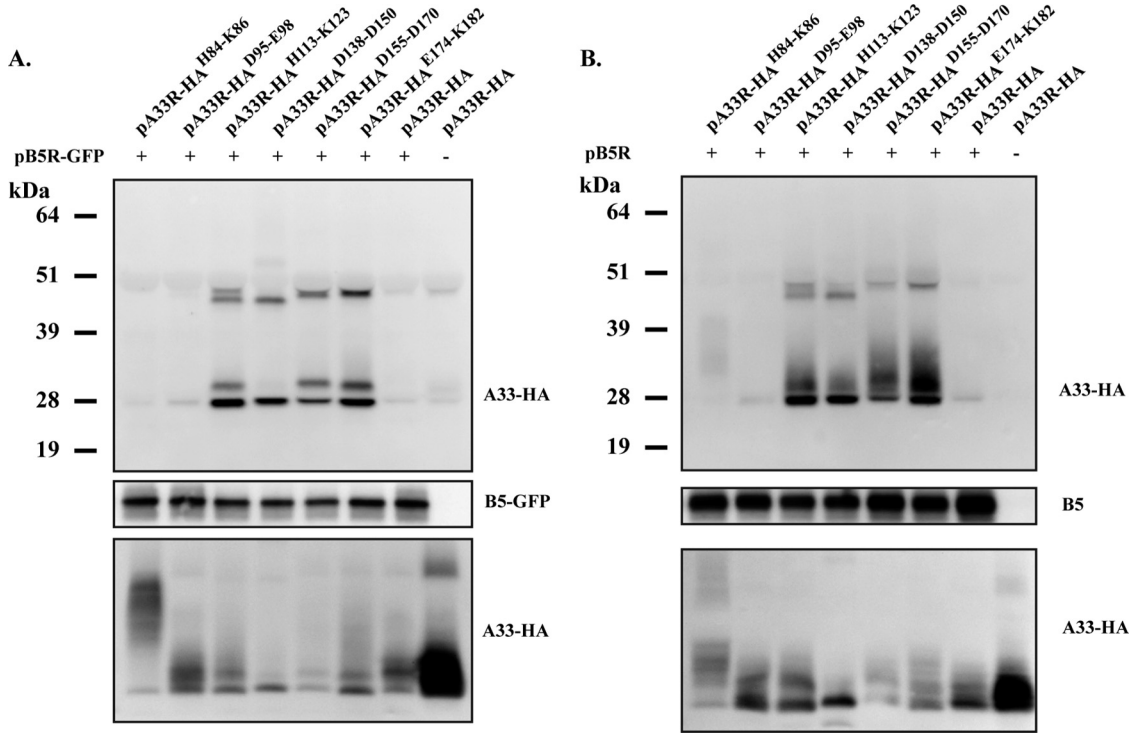

FIG 2 Group 2 A33 CTA mutant proteins have an increased interaction with both B5-GFP and B5. HeLa cells infected with vTF7.3 were transfected in the presence of AraC with the indicated plasmids encoding A33 CTA mutant proteins and either B5-GFP (A) or B5 (B). At 24 h posttransfection, cells were harvested and lysed in RIPA buffer. Cell lysates were subjected to immunoprecipitation with an anti-B5 antibody. Antibody-protein complexes were resolved by SDS-PAGE, followed by Western blotting with anti-HA MAb (top blots). Cell lysates were analyzed by Western blot assay using an anti-B5 antibody (middle blots) and anti-HA MAb (bottom blots) to examine the B5-GFP/B5 and A33 expression levels, respectively. The molecular masses, in kilodaltons, and positions of marker proteins are shown on the left.

with the anti-HA antibody. For this initial assay, proteins were radiolabeled because we were unsure if sufficient amounts of B5-GFP would interact with A33 for detection by Western blot assay. In addition, radiolabeling allowed us to assess the amount of each protein immunoprecipitated in our assay without detection using antibodies. All of the CTA mutant proteins tested were still able to precipitate B5-GFP (Fig. 1C). However, we noticed that, compared to A33-HA, the CTA mutant proteins fell into two groups; group 1 mutant proteins coimmunoprecipitated similar amounts of B5-GFP (A33R-HA$^{H84-K86}$ and A33R-HA$^{D95-E98}$), and group 2 mutant proteins coimmunoprecipitated more B5-GFP (A33R-HA$^{H113-K123}$, A33R-HA$^{D138-D150}$, A33R-HA$^{D155-D170}$, and A33R-HA$^{E174-K182}$) (Fig. 1C). We also observed that the majority of the group 2 mutant proteins migrated as a doublet, which is consistent with a hyperglycosylated form of A33 (Fig. 1C). Importantly, comparable amounts of the CTA mutant proteins were precipitated by the anti-HA MAb (Fig. 1C). To ensure that the increased level of B5-GFP that coimmunoprecipitated was not due to differences in B5-GFP expression levels, Western blot analysis of cell lysates was performed using an anti-GFP antibody. While the expression levels of B5-GFP did vary, importantly, they were not higher in cells in which the mutant proteins that fall into group 2 were coexpressed (Fig. 1C).

To confirm the previous result and be certain that the increased amount of B5-GFP that was precipitated was due to an increase in interaction and not to differences between the affinities of the anti-HA MAb for the mutant proteins we made, we repeated the CoIP using an antibody against B5 and analyzed the precipitate by probing for the HA epitope tag on our mutant proteins. Analogous to the previous results, the CTA mutant proteins in group 2 were precipitated with B5-GFP to a greater level than A33-HA and the mutant proteins in group 1 (Fig. 2A).

A33 has been shown to interact with both B5 and chimeric B5-GFP during infection (3, 4, 25). While B5-GFP requires an interaction with A33 for incorporation into virions, B5 does not (3, 4, 25). We wanted to determine if the group 2 CTA mutant proteins had an increased interaction with B5, as was seen with B5-GFP. Therefore, the CoIP was repeated using B5 in place of B5-GFP. B5 gave results identical to those obtained with B5-GFP (Fig. 2B), demonstrating that the group 2 CTA mutant proteins have increased interaction with both B5 and B5-GFP in our assay and that the increased interaction is independent of GFP.

Characterization of recombinant viruses expressing an A33R CTA mutant protein. Our efforts to map the residues in the lumenal domain of A33 that interact with B5 led to the interesting finding that certain A33 CTA mutant proteins had an increased interaction with B5 (Fig. 1C and 2). We wanted to examine if the increased interaction between A33 and B5-GFP had an effect on viral morphogenesis. Therefore, we generated recombinant viruses expressing B5R-GFP and the A33R CTA mutant proteins in place of normal B5 and A33R, respectively. These recombinants express B5R-GFP in place of normal B5R because B5-GFP has been shown to be more sensitive to defects in A33 (5). To characterize the recombinant viruses, we first examined the plaques pro-

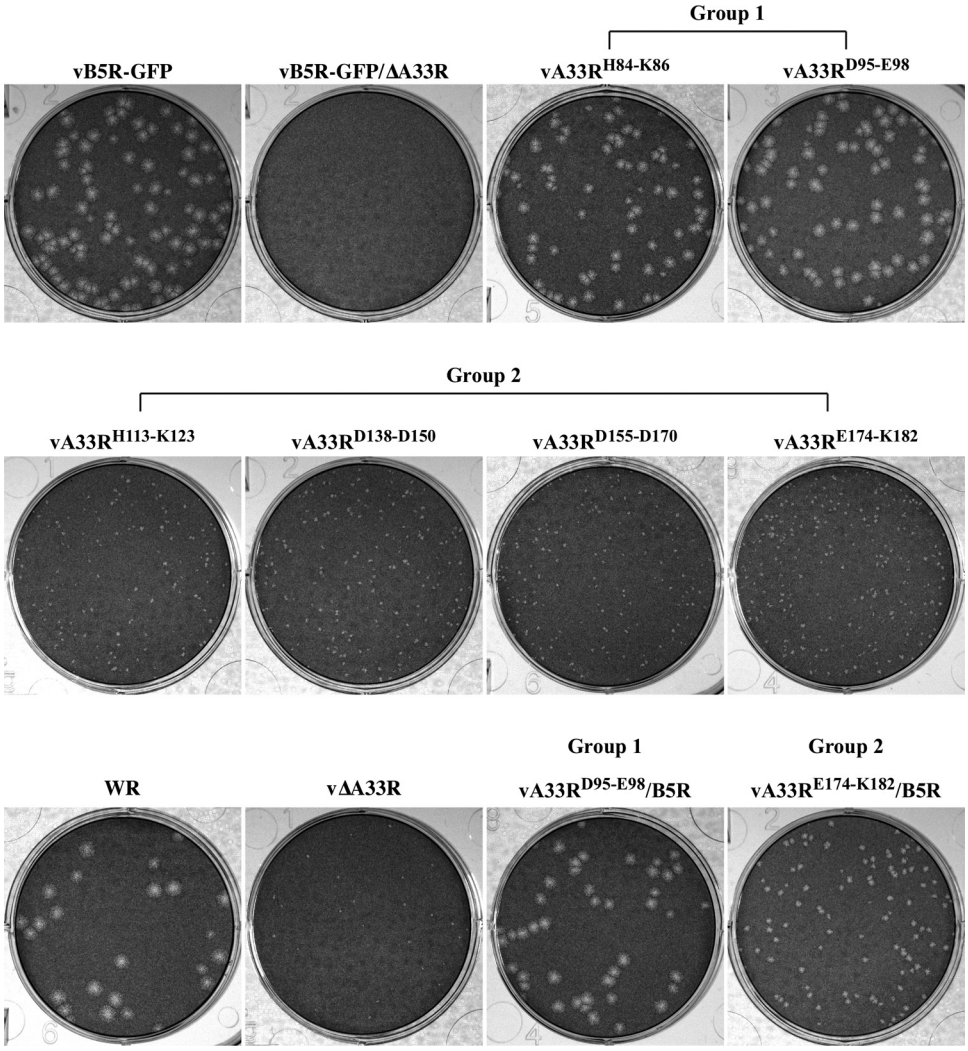

FIG 3 Plaque phenotypes of recombinant viruses expressing A33R CTA mutant proteins. Confluent BSC-1 cell monolayers were infected with the indicated viruses. At 2 h p.i., the inoculum was removed and cells were overlaid with semisolid medium. At 3 days p.i., cell monolayers were stained with crystal violet and imaged.

duced by the mutants and compared them to the plaques produced by the normal virus (vB5R-GFP) and a virus that has A33R deleted (vB5R-GFP/ΔA33R). The plaque assay showed that the recombinant viruses expressing an A33R CTA mutant protein that had a normal interaction with B5-GFP (group 1) made plaques that were similar in size to those made by vB5R-GFP (Fig. 3). In contrast, the recombinants expressing an A33R CTA mutant protein that had an increased interaction with B5-GFP (group 2) made plaques that were noticeably smaller than those made by vB5R-GFP but larger than those made by vB5R-GFP/ΔA33R (Fig. 3).

We wanted to ensure that the defect of group 2 mutants was due to the mutations in A33 and not B5-GFP. Therefore, we generated recombinant viruses expressing an A33R CTA mutant protein in a WR background that does not express GFP. We chose one mutant from each group, vA33R$^{D95\text{-}E98}$ (group 1) and vA33R$^{E174\text{-}K182}$ (group 2), and replaced B5R-GFP with B5R to generate vA33R$^{D95\text{-}E98}$/B5R and vA33R$^{E174\text{-}K182}$/B5R. As shown in Fig. 3, vA33R$^{D95\text{-}E98}$/B5R produced normal-sized plaques while vA33R$^{E174\text{-}K182}$/B5R produced small plaques, indicating that vA33R$^{E174\text{-}K182}$/B5R is defective regardless of whether B5R-GFP or B5R is expressed. Compared to vA33R$^{E174\text{-}K182}$ expressing B5R-GFP, vA33R$^{E174\text{-}K182}$/B5R made slightly larger plaques (Fig. 3), indicating that the recombinant viruses expressing an A33R CTA mutant protein in the B5R-GFP background are more sensitive to the mutations in A33. Therefore, we continued the characterization of the recombinant viruses in the vB5R-GFP background only.

A33 CTA mutant proteins localize properly during infection. To further define where the defect was occurring in recombinant viruses expressing a group 2 mutant protein, we examined, at the subcellular level, the localization of the A33 CTA mutant proteins during infection. We performed immunofluorescence microscopy of infected cells using rabbit anti-A33 antiserum, followed by Texas Red-conjugated donkey anti-rabbit antibody. We compared the localization of A33 in cells infected with a recombinant virus expressing an A33R CTA mutant protein to that seen in cells infected with either vB5R-GFP or vB5R-GFP/ΔA33R. During in-

fection, all of the A33 CTA mutant proteins localized to the site of wrapping and to the cell vertices (Fig. 4). In addition, A33-stained virion-sized particles were observed in the cell periphery (Fig. 4). Therefore, our immunofluorescence microscopy indicated that all of the A33 CTA mutant proteins localized properly and were incorporated into progeny enveloped virions. During normal infection, B5-GFP has been shown to localize at the site of wrapping, on virion-sized particles in the cytoplasm, and at the cell vertices (45). In contrast, we have shown that in the absence of A33, B5-GFP is mislocalized, with GFP fluorescence seen only at the site of wrapping, indicating that A33 is required for proper targeting of B5-GFP (5). We therefore examined if B5-GFP was properly localized in cells infected with a recombinant virus expressing a group 2 mutant protein. We found that in cells infected with a recombinant virus that makes small plaques, B5-GFP localized to the site of wrapping but failed to accumulate at the cell vertices. Although virion-sized particles labeled with A33 were observed in cells infected with a recombinant virus expressing a group 2 mutant protein, distinct virion-sized particles labeled with GFP were not observed (Fig. 4). In contrast, B5-GFP localization in cells infected with a recombinant virus expressing a group 1 mutant protein was indistinguishable from that seen in cells infected with vB5R-GFP (Fig. 4).

Cell-associated EV produced by recombinant viruses expressing an A33R CTA mutant protein is capable of inducing actin tails. Plaque size, which represents the ability of orthopoxviruses to spread from cell to cell, is directly related to the amount of infectious EV produced and their ability to induce actin tails (34, 44). We wanted to examine if the cell-associated EV (CEV) produced by a group 2 mutant was capable of inducing actin tails. We therefore visualized virus-induced actin tails, as well as B5-GFP incorporation into CEV, using immunofluorescence microscopy. Unpermeabilized cells infected with vB5R-GFP, vB5R-GFP/ΔA33R, or a virus expressing an A33R CTA mutant protein were immunostained with an anti-B5 MAb, followed by permeabilization and subsequent staining with Alexa Fluor 350-conjugated phalloidin to visualize virus-induced actin tails. On the surface of cells infected with either vB5R-GFP or any of the recombinant viruses expressing an A33R CTA mutant protein, B5-labeled virion-sized particles and actin tails underneath the B5-labeled CEV were observed, although less frequently on cells infected with a recombinant virus expressing a group 2 mutant protein (Fig. 5). As had been shown previously, on the surface of cells infected with vB5R-GFP/ΔA33R, neither B5-labeled virion-sized particles nor virus-induced actin tails were observed (Fig. 5) (5). Therefore, our data indicate that B5-GFP is incorporated into CEV and that CEV produced by a recombinant virus expressing a group 2 mutant protein are capable of inducing actin tails. While distinct virion-sized particles labeled with B5-GFP were not observed in the cytoplasm of cells infected with a recombinant virus expressing a group 2 mutant protein (Fig. 4), surface staining with an anti-B5 MAb showed that B5-GFP localized to virion-sized particles, consistent with CEV, on the cell surface (Fig. 5). It is possible that the strong B5-GFP fluorescence in the cytoplasm of cells infected with a recombinant virus expressing a group 2 CTA mutant protein masked the signal of B5-GFP-labeled virion-sized particles.

Group 2 CTA mutant proteins are incorporated into CEV. We next wanted to examine the incorporation of the A33 CTA mutant proteins into EV. Therefore, we stained cells infected with vB5R-GFP, vB5R-GFP/ΔA33R, or a recombinant virus expressing an A33R CTA mutant protein with a rabbit anti-A33 antiserum without permeabilization. After staining with an anti-A33 antibody, filamentous actin was stained with Alexa Fluor 350-conjugated phalloidin. As expected, A33 staining was found on the surface of cells infected with each of the recombinant viruses, with the exception of vB5R-GFP/ΔA33R (Fig. 6). In addition, actin tails beneath A33-stained virion-sized particles were observed, indicating that A33 is incorporated into CEV produced by all of the A33R CTA recombinant viruses (Fig. 6). So far, the mutants within each group have similar characteristics in the previous assays performed, indicating that the recombinant viruses in each group behave similarly. Therefore, further characterization of our recombinant viruses was carried out with only a representative mutant from each group, i.e., vA33R$^{D95\text{-}E98}$ (group 1) or vA33R$^{E174\text{-}K182}$ (group 2).

The increased interaction between A33 and B5-GFP during infection correlates with a small-plaque phenotype. Our plaque assay shows that a recombinant virus expressing a group 2 CTA mutant protein makes small plaques (Fig. 3). The interaction between A33 and B5 is easily detected using the T7 expression system, whereas during infection, the interaction is less robust (4). We wanted to determine if an increased interaction between a group 2 CTA mutant protein and either B5 or B5-GFP could be detected during infection. Therefore, we examined the interaction between A33 and B5/B5-GFP in infected cells using CoIP. Consistent with our initial CoIP performed using the overexpression system (Fig. 1), a band corresponding to either B5 or B5-GFP was coimmunoprecipitated with A33 from the lysates of cells infected with a recombinant virus expressing the group 2 CTA mutant protein (Fig. 7A). An ~51-kDa nonspecific band was detected in all of the samples and likely represents the heavy chain from the antibodies used to perform the precipitation. These results show that there is an increased interaction between A33 group 2 CTA mutant proteins and both B5 and B5-GFP during infection. In contrast, undetectable amounts of B5/B5-GFP were coimmunoprecipitated with A33 from the lysates of cells infected with a recombinant virus expressing a group 1 mutant protein, vB5R-GFP, or vB5R-GFP/ΔA33R or mock infected (Fig. 7A). Therefore, our data indicate that the increased A33-B5 interaction correlates with the small-plaque phenotype and suggest normally that the interaction between A33 and B5/B5-GFP during infection is either transient or weak.

A33R group 2 CTA mutant proteins increase the interaction between A33 and B5-GFP on the surface of EV. Our previous results indicated a correlation between an increased A33-B5 interaction and a small-plaque phenotype (Fig. 3 and 7A). We hypothesized that given the stronger interaction, the A33/B5-GFP complex could persist on the surface of EEV released from cells infected with a recombinant virus expressing a group 2 CTA mutant protein and that the prolonged interaction on the EV surface may be detrimental to subsequent infection. To test this idea, lysates of purified radiolabeled virions released into the medium were subjected to immunoprecipitation with an anti-B5 MAb, anti-A33 rabbit antiserum, or an anti-F13 MAb (as a control). As shown in Fig. 7B, a band corresponding to B5-GFP or A33 was detected in the lysates of EEV released by cells infected with vB5R-GFP and recombinant viruses expressing a group 1 or 2 mutant. F13 was immunoprecipitated from the lysates of EEV released by cells infected with any of the recombinant viruses (Fig. 7B). The group 2 CTA mutant protein A33$^{E174\text{-}K182}$ migrated as a smear (Fig. 7B). Regardless, more B5-GFP was coimmunoprecipitated

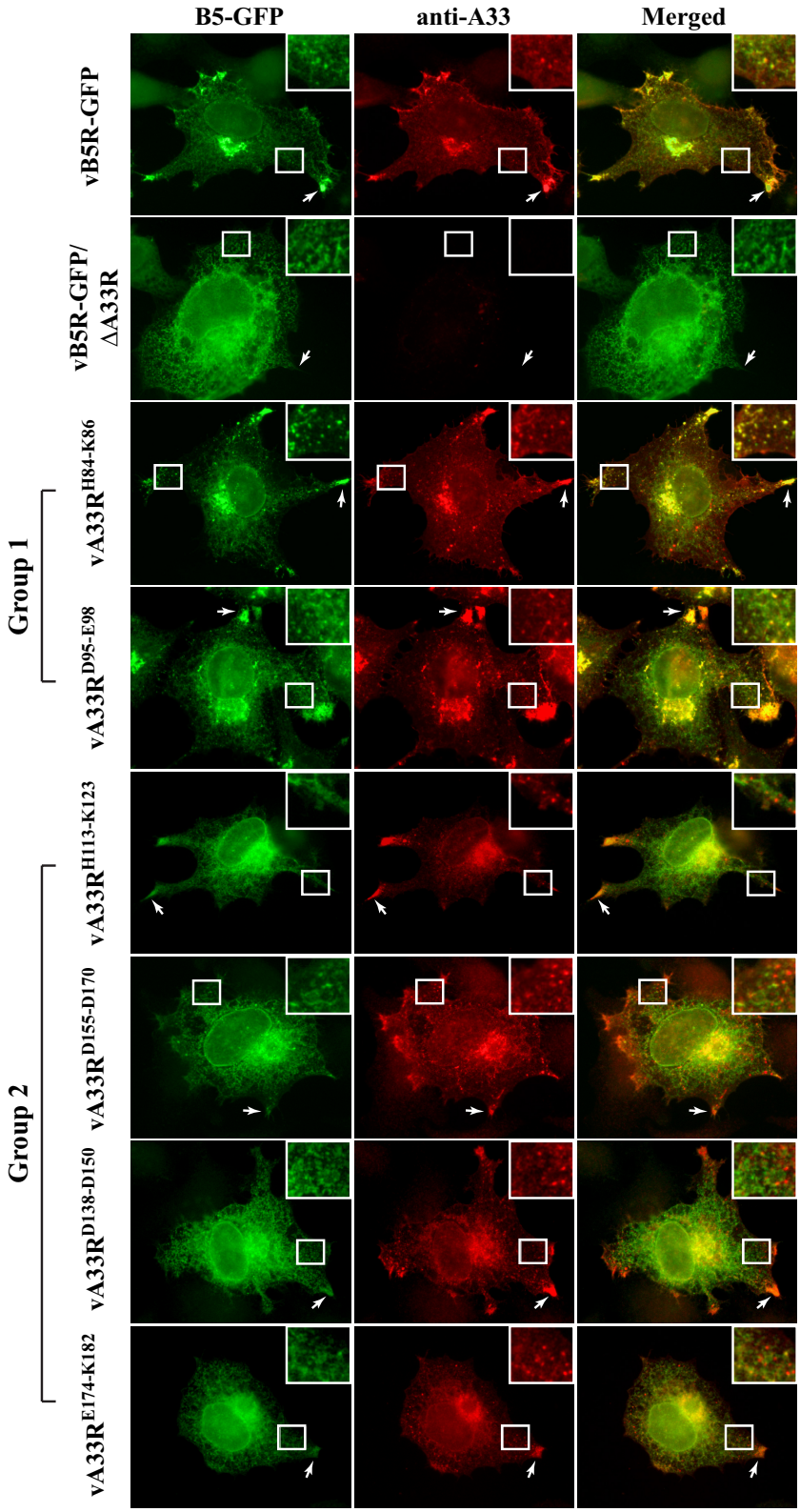

FIG 4 A33 CTA mutant proteins localize properly during infection. HeLa cells grown on glass coverslips were infected with the indicated viruses. The next day, fixed and permeabilized cells were stained with rabbit anti-A33 antiserum, followed by Texas Red-conjugated donkey anti-rabbit antibody. The overlap of B5-GFP (green) and A33 (red) is yellow. Arrows indicate the accumulation of B5-GFP and/or A33 at the cell vertices. Boxed regions are enlarged in the upper right corners to highlight virion-sized particles.

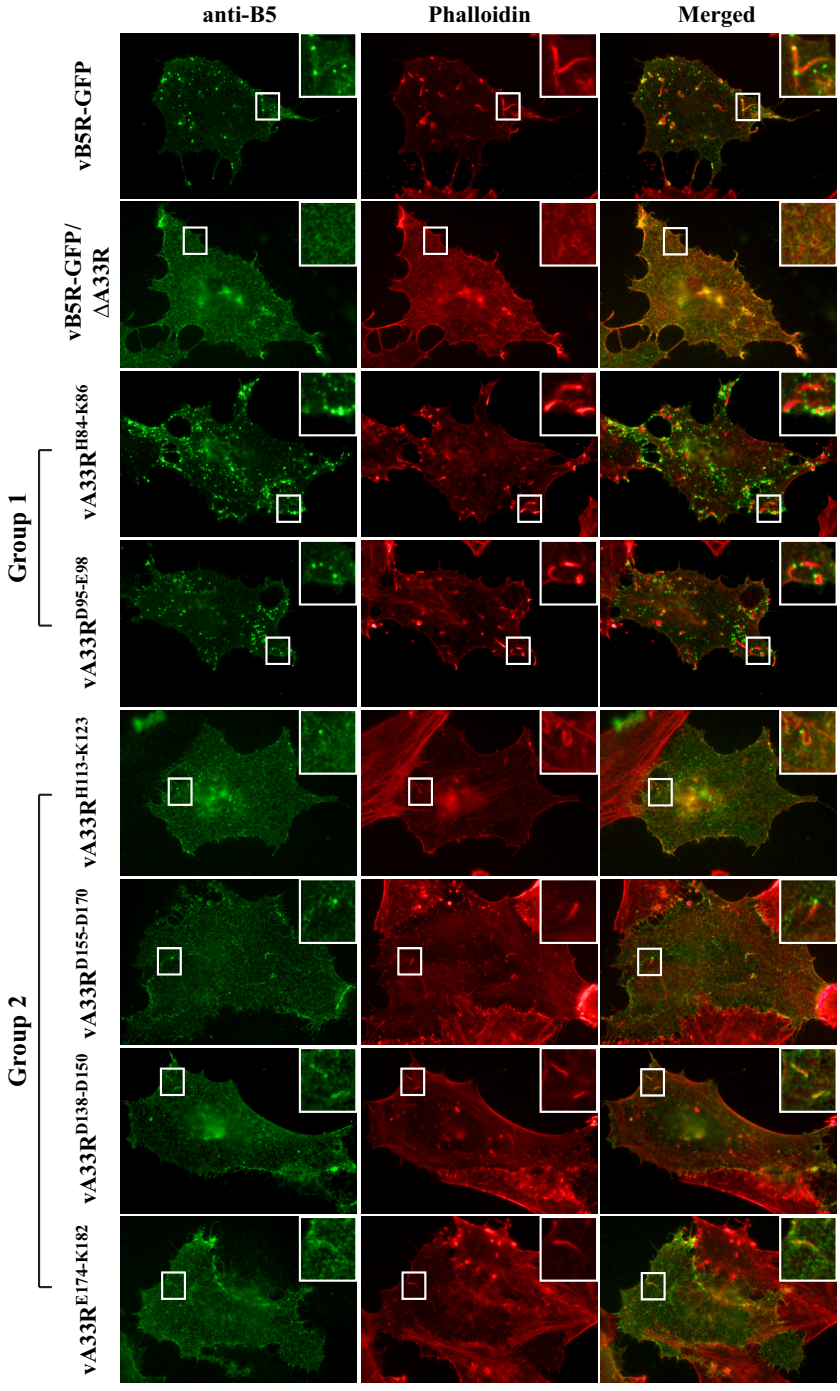

FIG 5 Actin tails are induced by CEV made by recombinant viruses expressing A33R CTA mutant proteins. HeLa cells grown on glass coverslips were infected with the indicated viruses. The next day, fixed cells were stained with an anti-B5 MAb, followed by Texas Red-conjugated donkey anti-rat antibody (shown as green). After staining, cells were permeabilized and filamentous actin was stained with Alexa Fluor 350-conjugated phalloidin (shown as red). The overlap of B5 surface staining (green) and actin tails (red) is yellow. Boxed regions are enlarged in the upper right corners to highlight actin tails beneath B5-labeled CEV.

with A33 from the lysate of EEV released by cells infected with a recombinant virus expressing a group 2 mutant protein than from the lysates of EEV released by cells infected with either a recombinant virus expressing a group 1 mutant protein or vB5R-GFP (Fig. 7B). This indicates that A33 and B5-GFP still exist as a complex on the surface of EEV released by cells infected with a recombinant virus that makes small plaques.

The presence of the A33-B5 complex on the surface of EEV reduces the cell binding ability of EEV. We have shown that A33 is required for efficient binding of EV to target BSC-1 cells (5). We hypothesized that the presence of the A33-B5 complex on the surface of EEV would affect the binding ability of EEV and that this could cause the reduction seen in the plaque size of the virus producing CTA mutant proteins. Therefore, we quantified the

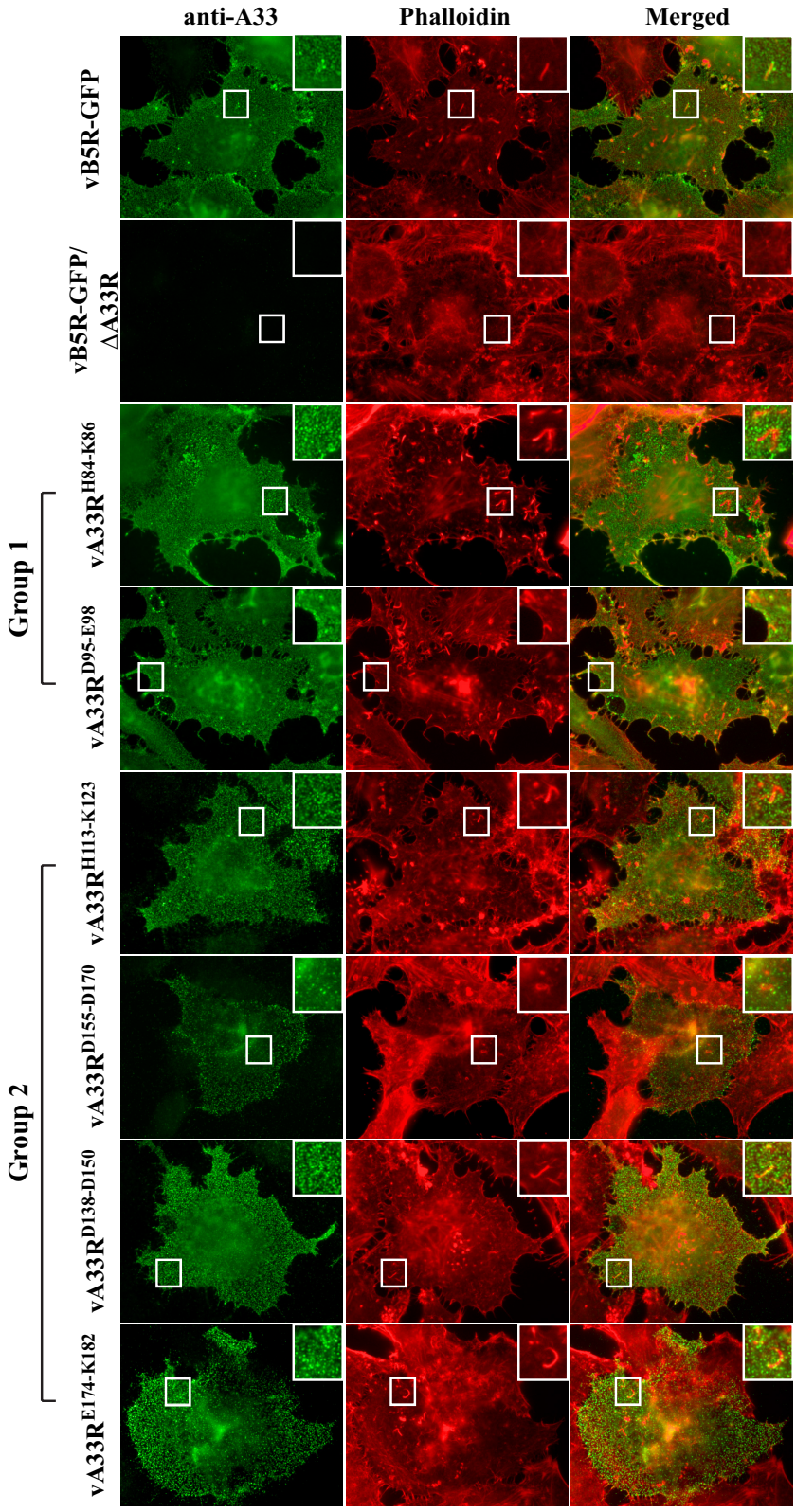

FIG 6 A33 CTA mutant proteins are incorporated into CEV. HeLa cells grown on glass coverslips were infected with the indicated viruses. The next day, fixed cells were stained with a rabbit anti-A33 antiserum, followed by Texas Red-conjugated donkey anti-rabbit antibody (shown as green). After staining, cells were permeabilized and filamentous actin was stained with Alexa Fluor 350-conjugated phalloidin (shown as red). The overlap of A33 surface staining (green) and actin tails (red) is yellow. Boxed regions are enlarged in the upper right corners to highlight actin tails beneath A33-labeled CEV.

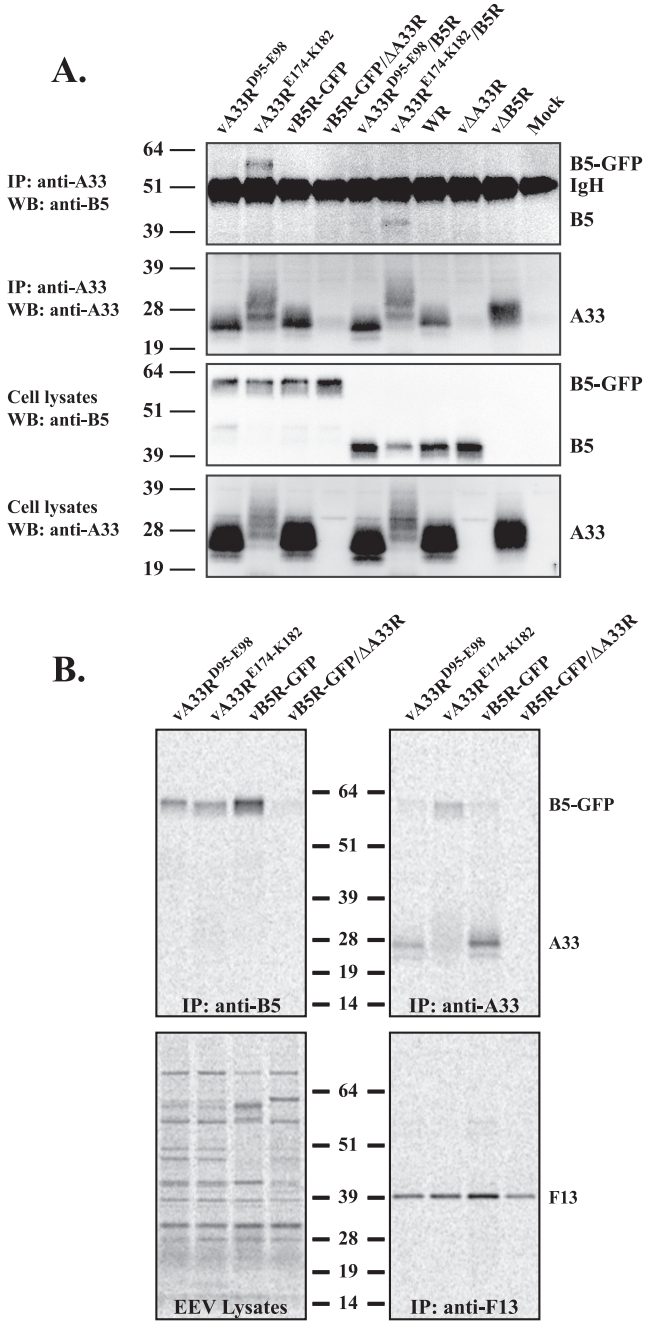

FIG 7 A33 and B5-GFP exist as a complex on the surface of EEV produced by a recombinant virus expressing a group 2 mutant protein. (A) CoIP. HeLa cells were infected with the indicated viruses, and the next day, cells were harvested and lysed in RIPA buffer. Cell lysates were subjected to immunoprecipitation (IP) with an anti-A33 rabbit antiserum. Antibody-protein complexes or cell lysates were resolved by SDS-PAGE. Western blotting (WB) was performed using an anti-B5 MAb, followed by HRP-conjugated donkey anti-rat antibody. Afterward, blots were stripped and reprobed with an anti-A33 rabbit antiserum, followed by an HRP-conjugated donkey anti-rabbit antibody. The heavy chain from the precipitating antibody is indicated as IgH. (B) Analysis of EEV. Lysates of purified radiolabeled EEV released from RK_{13} cells infected with the indicated viruses were subjected to immunoprecipitation with an anti-B5 MAb, anti-A33 rabbit antiserum, or an anti-F13 MAb. Antibody-protein complexes were resolved by SDS-PAGE, and proteins were detected by autoradiography. Equilibrated EEV lysates were analyzed to show that the same amount of EEV was used for immunoprecipitation. The molecular masses, in kilodaltons, and positions of marker proteins are shown.

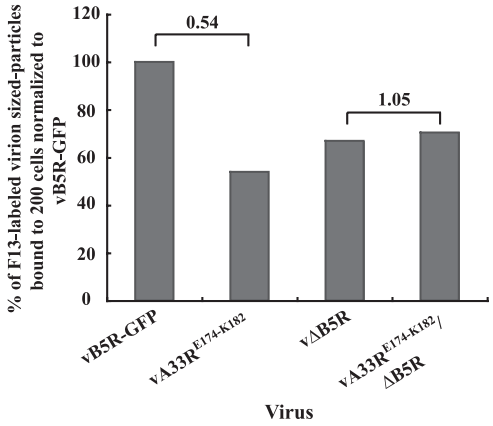

FIG 8 The presence of the A33-B5 complex on the surface of EEV reduces the ability of EEV to bind to target cells. HeLa cells grown on glass coverslips were inoculated on ice with the indicated viruses that had been equilibrated by real-time PCR. Fixed and permeabilized cells were stained with an anti-F13 antibody, followed by Texas Red-conjugated donkey anti-mouse antibody. The binding ability of EEV was determined by counting the F13-labeled virion-sized particles that were bound to 200 cells. The average of two independent experiments was determined and is shown as a percentage normalized to vB5R-GFP. The *n*-fold differences between the bracketed columns are shown at the top.

amount of EEV produced by either vB5R-GFP or a recombinant virus expressing a group 2 CTA mutant protein using real-time PCR. We found that $vA33R^{E174\text{-}K182}$ and vB5R-GFP released similar amounts of genome copies from infected cells (data not shown), indicating that neither the CTA mutation in A33 nor the prolonged interaction with B5-GFP was deleterious to EV formation. Using the real-time PCR results for equilibration, we added the same number of EEV to HeLa cells and determined the number of virions bound by quantifying virion-sized particles labeled with F13. As shown in Fig. 8, the number of EEV produced by a recombinant virus expressing a group 2 mutant protein that was bound to cells was about 2-fold lower than that of EEV produced by vB5R-GFP, indicating that the presence of A33-B5 complexes on the surface of EEV reduces the ability of EEV to bind target cells.

We next wanted to confirm that the reduced cell binding of EEV produced by a recombinant virus expressing a group 2 mutant protein was due to the increased presence of the A33-B5 complex and not to any effect the mutations might have on the intrinsic binding ability of A33. Therefore, we constructed a recombinant virus that expresses $A33R^{E174\text{-}K182}$ in the absence of B5 and compared its binding ability to that of wild-type A33 in the absence of B5. The amount of EEV produced by $vA33R^{E174\text{-}K182}$/ΔB5R that were bound to cells was the same as that of EEV produced by vΔB5R (Fig. 8), indicating that EEV produced by $vA33R^{E174\text{-}K182}$/ΔB5R bind cells as efficiently as those produced by vΔB5R, which contains normal A33. Therefore, our data demonstrate that the reduced binding of EEV produced by a recombinant virus expressing a group 2 mutant protein is due to the presence of A33-B5 as a complex and not to the inability of mutant A33 to bind cells.

DISCUSSION

The interaction between A33 and B5, in the absence of other viral late proteins and during infection, has been previously reported

(3, 4, 25), yet the significance of the interaction is unclear because in the absence of A33, B5 is still found in EV released from the cell. In contrast, B5-GFP requires A33 for incorporation into EV, suggesting that there are two pathways for the incorporation of B5 into virions released from the cell, one of which requires A33 (5). We have found that the lumenal domain of A33 is sufficient for interaction with both B5 and B5-GFP (4). Our attempt to identify the interacting residues in A33 with B5 led us to an interesting investigation of the role of the A33-B5 interaction during infection. We isolated A33 CTA mutant proteins that have an increased interaction with both B5-GFP and B5 (Fig. 2). Recombinant viruses expressing these mutant proteins did not make normal-sized plaques (Fig. 3) in the presence of either B5 or B5-GFP. However, the recombinant virus expressing B5 did make plaques that were noticeably bigger than those that expressed B5-GFP. This subtle difference in plaque size is most likely the result of some B5 incorporated into IEV in an A33-independent way for the recombinant that expresses normal B5R. This B5 would not be in a complex with A33, and therefore, these EV should be more infectious. This would confirm previous findings that B5 has a role not only in IEV formation (12, 18) but also in the infectivity of EV (5, 20) and suggests that the interaction between B5 and A33 should be transient for full functionality during infectivity. In addition, the fact the vA33R$^{E174\text{-}K182}$ that expresses normal B5R also has a reduction in plaque size indicates that the A33-dependent mechanism not only functions during normal infection but may be the predominant pathway for the incorporation of B5 into EV. If A33-dependent incorporation of B5-GFP is the predominant pathway for its incorporation, then that would explain why vB5R-GFP produces plaques that are identical in size to those produced by WR and no defect is seen in vB5R-GFP.

We can think of two possibilities as to why the group 2 mutants have a more durable interaction with B5. First, the mutations cause a stronger interaction with B5. It is possible that the loss of charge is causing the structure of A33 to be less rigid and thus allows increased interaction with B5. Indeed, the hyperglycosylation of these mutant proteins (Fig. 1C) suggests that they provide greater access to residues that are typically not glycosylated, indicating a more relaxed A33 structure. A second possibility is that the mutations have affected A33 such that it is less able to dissociate with B5 and therefore the interaction is prolonged. It should be noted that the A33-B5 interaction was readily detected in the absence of other viral late proteins using the vaccinia virus T7 expression system (Fig. 1C and 2). Under similar conditions, the interaction was not easily detected during a normal infection when all of the viral proteins were present (Fig. 7A). In addition, we detected little to no A33-B5 complex on the surface of normal virions (Fig. 7B). This suggests that the A33-B5 interaction is either transient or weak when other viral late proteins are present and morphogenesis is occurring. If the interaction is transient, it is unclear what the mechanism is for the dissociation of B5 from A33 or where it occurs. One possibility is that a third protein interacts with A33 and causes it to dissociate with B5. Our mutations may have affected the ability of A33 to interact with this hypothetical protein and thus prevents the dissociation of the A33-B5 complex.

Interactions between the following IEV-specific proteins have been described: A33 and A36 (46), A33 and B5 (25), A33 and F13 (25), A34 and B5 (10, 26), A34 and A36 (31), F13 and B5 (6, 24), A36 and F12 (19), and E2 and F12 (17). Some of these interactions have been shown to be required for the coordinated incorporation of proteins into the envelope of IEV/EV. One example, the A33-A36 interaction, is required for the incorporation of A36 into the wrapping membrane (46, 49). The same region of A36 that interacts with A33 also interacts with the microtubule motor kinesin, and the interactions are mutually exclusive (46). It has been suggested that this interaction ensures that only completely wrapped IEV are transported along microtubules for egress (46). Taken together, our data suggest that protein-protein interactions that occur during poxvirus morphogenesis need to be tightly regulated for the production of fully infectious enveloped virions. This tight regulation is most likely achieved by an interaction cascade that occurs during intracellular envelopment. Such an interaction cascade involving A33, A36, and the microtubule motor kinesin has been suggested to occur (41, 43).

All of the recombinant viruses expressing a group 2 mutation in A33 had a small-plaque phenotype. Intuitively, several factors could contribute to the size of the plaques formed on cell monolayers by vaccinia virus, including, the number of EV formed, their ability to form actin tails, and their ability to bind cells. We found that the group 2 mutants did not profoundly affect the amount of EV released (data not shown). However, we did notice that these mutants appear to make fewer actin tails, a process that requires the incorporation and phosphorylation of the viral protein A36 (13). As the incorporation of A36 into the IEV membrane requires an interaction with A33 (49), a decrease in actin tails could be the result of an altered interaction with A36 by these mutants. In addition, B5 has been reported to be involved in an outside-in signaling cascade that results in the phosphorylation and subsequent activation of A36 (23). It is just as likely that an increased interaction with A33 may adversely affect this cascade and reduce the number of actin tails formed. Regardless, if either or both of these occur, a reduction in actin tail formation cannot fully account for the decrease in plaque size demonstrated by viruses producing the group 2 CTA mutant proteins because a full abrogation of actin tail formation results in an only ~30% decrease in plaque size (44). This suggested that the group 2 CTA mutant proteins may have reduced cell binding. Indeed, half as many EEV produced by vA33R$^{E174\text{-}K182}$ as those produced by vB5R-GFP bound cells. It seems likely that both of these defects contribute to the reduction in plaque size produced by recombinants expressing a group 2 CTA mutant protein.

A33 has been shown to be involved in efficient target cell binding (5). Our investigation into the binding ability of EEV produced by vΔB5R indicates that EEV lacking B5 can still bind cells, although at reduced levels, compared to that of EEV produced by vB5R-GFP (Fig. 8), suggesting a role for B5 in target cell binding. We previously reported that A33 is required for EEV to bind target cells efficiently while B5 plays a minor role in cell binding because the lack of B5, in addition to A33, does not further reduce the binding ability of EEV (5). This raises the possibility that B5 and A33 mediate cooperative target cell binding. A34 and B5 have been shown to be present as a complex on the surface of EEV (27). It has also been reported that in the absence of B5, A34 is present at a reduced level (2). Based on the report by Breiman and Smith, one would predict that less A34 is incorporated into EEV in the absence of B5 than in its presence (2). Importantly, the extracellular domain of A34 has been predicted to contain a C-type lectin-like domain. Indeed, A34 has been shown to be required for the retention of CEV on the cell surface (8). Therefore, it is tempting to speculate that the reduced binding ability of EEV produced by

vΔB5R is due to the presence of less A34 and not to the lack of B5. We have found that the aberrant A33-B5 interaction on the surface of EEV reduces the binding ability of those EEV (Fig. 8). Our examination of the ability of EEV produced by vA33R$^{E174-K182}$/ΔB5R in comparison with that of EEV produced by vΔB5R demonstrates that, for efficient cell binding, B5 and A33 cannot be present as a complex on the surface of EEV (Fig. 8). It will be of interest to determine the spatial and temporal regulation of all of the interactions between the various IEV-specific proteins during vaccinia virus infection, morphogenesis, egress, and subsequent cell binding.

ACKNOWLEDGMENTS

We thank Jay Hooper for an anti-F13 MAb.

This work was supported in part by NIH AI067391 research grant. W.M.C. was supported by National Institute of Allergy and Infectious Diseases Molecular Pathogenesis of Bacteria and Viruses Training Grant T32 AI007362.

REFERENCES

1. **Blasco R, Moss B.** 1991. Extracellular vaccinia virus formation and cell-to-cell virus transmission are prevented by deletion of the gene encoding the 37,000-dalton outer envelope protein. J. Virol. **65**:5910–5920.
2. **Breiman A, Smith GL.** 2010. Vaccinia virus B5 protein affects the glycosylation, localization and stability of the A34 protein. J. Gen. Virol. **91**: 1823–1827.
3. **Chan WM, Kalkanoglu AE, Ward BM.** 2010. The inability of vaccinia virus A33R protein to form intermolecular disulfide-bonded homodimers does not affect the production of infectious extracellular virus. Virology **408**:109–118.
4. **Chan WM, Ward BM.** 2012. The A33-dependent incorporation of B5 into extracellular enveloped vaccinia virions is mediated through an interaction between their lumenal domains. J. Virol. **86**:8210–8220.
5. **Chan WM, Ward BM.** 2010. There is an A33-dependent mechanism for the incorporation of B5-GFP into vaccinia virus extracellular enveloped virions. Virology **402**:83–93.
6. **Chen Y, et al.** 2009. Vaccinia virus p37 interacts with host proteins associated with LE-derived transport vesicle biogenesis. Virol. J. **6**:44.
7. **Condit RC, Moussatche N, Traktman P.** 2006. In a nutshell: structure and assembly of the vaccinia virion. Adv. Virus Res. **66**:31–124.
8. **Duncan SA, Smith GL.** 1992. Identification and characterization of an extracellular envelope glycoprotein affecting vaccinia virus egress. J. Virol. **66**:1610–1621.
9. **Earl PL, Moss B.** 1991. Generation of recombinant vaccinia viruses, p 16.17.11–16.17.16. *In* Ausubel FM, et al. (ed), Current protocols in molecular biology, vol 2. Greene Publishing Associates & Wiley Interscience, New York, NY.
10. **Earley AK, Chan WM, Ward BM.** 2008. The vaccinia virus B5 protein requires A34 for efficient intracellular trafficking from the endoplasmic reticulum to the site of wrapping and incorporation into progeny virions. J. Virol. **82**:2161–2169.
11. **Engelstad M, Howard ST, Smith GL.** 1992. A constitutively expressed vaccinia gene encodes a 42-kDa glycoprotein related to complement control factors that forms part of the extracellular virus envelope. Virology **188**:801–810.
12. **Engelstad M, Smith GL.** 1993. The vaccinia virus 42-kDa envelope protein is required for the envelopment and egress of extracellular virus and for virus virulence. Virology **194**:627–637.
13. **Frischknecht F, et al.** 1999. Actin-based motility of vaccinia virus mimics receptor tyrosine kinase signalling. Nature **401**:926–929.
14. **Fuerst TR, Niles EG, Studier FW, Moss B.** 1986. Eukaryotic transient-expression system based on recombinant vaccinia virus that synthesizes bacteriophage T7 RNA polymerase. Proc. Natl. Acad. Sci. U. S. A. **83**: 8122–8126.
15. **Herrera E, del Mar Lorenzo M, Blasco R, Isaacs SN.** 1998. Functional analysis of vaccinia virus B5R protein: essential role in virus envelopment is independent of a large portion of the extracellular domain. J. Virol. **72**:294–302.
16. **Hiller G, Weber K.** 1985. Golgi-derived membranes that contain an acylated viral polypeptide are used for vaccinia virus envelopment. J. Virol. **55**:651–659.
17. **Hume AN, Tarafder AK, Ramalho JS, Sviderskaya EV, Seabra MC.** 2006. A coiled-coil domain of melanophilin is essential for myosin Va recruitment and melanosome transport in melanocytes. Mol. Biol. Cell **17**:4720–4735.
18. **Isaacs SN, Wolffe EJ, Payne LG, Moss B.** 1992. Characterization of a vaccinia virus-encoded 42-kilodalton class I membrane glycoprotein component of the extracellular virus envelope. J. Virol. **66**:7217–7224.
19. **Johnston SC, Ward BM.** 2009. Vaccinia virus protein F12 associates with intracellular enveloped virions through an interaction with A36. J. Virol. **83**:1708–1717.
20. **Law M, Carter GC, Roberts KL, Hollinshead M, Smith GL.** 2006. Ligand-induced and nonfusogenic dissolution of a viral membrane. Proc. Natl. Acad. Sci. U. S. A. **103**:5989–5994.
21. **Mathew E, Sanderson CM, Hollinshead M, Smith GL.** 1998. The extracellular domain of vaccinia virus protein B5R affects plaque phenotype, extracellular enveloped virus release, and intracellular actin tail formation. J. Virol. **72**:2429–2438.
22. **Moss B.** 2001. *Poxviridae*: the viruses and their replication, p 2849–2883. *In* Fields BN, Knipe DM, Howley PM (ed), Fields virology, fourth ed, vol 2. Lippincott-Raven Publishers, Philadelphia, PA.
23. **Newsome TP, Scaplehorn N, Way M.** 2004. SRC mediates a switch from microtubule- to actin-based motility of vaccinia virus. Science **306**:124–129.
24. **Payne LG.** 1992. Characterization of vaccinia virus glycoproteins by monoclonal antibody preparations. Virology **187**:251–260.
25. **Perdiguero B, Blasco R.** 2006. Interaction between vaccinia virus extracellular virus envelope A33 and B5 glycoproteins. J. Virol. **80**:8763–8777.
26. **Perdiguero B, Lorenzo MM, Blasco R.** 2008. Vaccinia virus A34 glycoprotein determines the protein composition of the extracellular virus envelope. J. Virol. **82**:2150–2160.
27. **Roberts KL, et al.** 2009. Acidic residues in the membrane-proximal stalk region of vaccinia virus protein B5 are required for glycosaminoglycan-mediated disruption of the extracellular enveloped virus outer membrane. J. Gen. Virol. **90**:1582–1591.
28. **Roberts KL, Smith GL.** 2008. Vaccinia virus morphogenesis and dissemination. Trends Microbiol. **16**:472–479.
29. **Roper RL, Payne LG, Moss B.** 1996. Extracellular vaccinia virus envelope glycoprotein encoded by the A33R gene. J. Virol. **70**:3753–3762.
30. **Roper RL, Wolffe EJ, Weisberg A, Moss B.** 1998. The envelope protein encoded by the A33R gene is required for formation of actin-containing microvilli and efficient cell-to-cell spread of vaccinia virus. J. Virol. **72**: 4192–4204.
31. **Röttger S, Frischknecht F, Reckmann I, Smith GL, Way M.** 1999. Interactions between vaccinia virus IEV membrane proteins and their roles in IEV assembly and actin tail formation. J. Virol. **73**:2863–2875.
32. **Schmelz M, et al.** 1994. Assembly of vaccinia virus: the second wrapping cisterna is derived from the trans Golgi network. J. Virol. **68**:130–147.
33. **Shida H.** 1986. Nucleotide sequence of the vaccinia virus hemagglutinin gene. Virology **150**:451–462.
34. **Smith GL, Vanderplasschen A, Law M.** 2002. The formation and function of extracellular enveloped vaccinia virus. J. Gen. Virol. **83**:2915–2931.
35. **Su HP, Singh K, Gittis AG, Garboczi DN.** 2010. The structure of the poxvirus A33 protein reveals a dimer of unique C-type lectin-like domains. J. Virol. **84**:2502–2510.
36. **Tooze J, Hollinshead M, Reis B, Radsak K, Kern H.** 1993. Progeny vaccinia and human cytomegalovirus particles utilize early endosomal cisternae for their envelopes. Eur. J. Cell Biol. **60**:163–178.
37. **Turner PC, Moyer RW.** 2006. The cowpox virus fusion regulator proteins SPI-3 and hemagglutinin interact in infected and uninfected cells. Virology **347**:88–99.
38. **van Eijl H, Hollinshead M, Rodger G, Zhang WH, Smith GL.** 2002. The vaccinia virus F12L protein is associated with intracellular enveloped virus particles and is required for their egress to the cell surface. J. Gen. Virol. **83**:195–207.
39. **van Eijl H, Hollinshead M, Smith GL.** 2000. The vaccinia virus A36R protein is a type Ib membrane protein present on intracellular but not extracellular enveloped virus particles. Virology **271**:26–36.
40. **Wagenaar TR, Moss B.** 2007. Association of vaccinia virus fusion regulatory proteins with the multicomponent entry/fusion complex. J. Virol. **81**:6286–6293.

41. **Ward BM.** 2005. The longest micron; transporting poxviruses out of the cell. Cell. Microbiol. **7**:1531–1538.
42. **Ward BM.** 2005. Visualization and characterization of the intracellular movement of vaccinia virus intracellular mature virions. J. Virol. **79**:4755–4763.
43. **Ward BM, Moss B.** 2004. Vaccinia virus A36R membrane protein provides a direct link between intracellular enveloped virions and the microtubule motor kinesin. J. Virol. **78**:2486–2493.
44. **Ward BM, Moss B.** 2001. Vaccinia virus intracellular movement is associated with microtubules and independent of actin tails. J. Virol. **75**: 11651–11663.
45. **Ward BM, Moss B.** 2001. Visualization of intracellular movement of vaccinia virus virions containing a green fluorescent protein-B5R membrane protein chimera. J. Virol. **75**:4802–4813.
46. **Ward BM, Weisberg AS, Moss B.** 2003. Mapping and functional analysis of interaction sites within the cytoplasmic domains of the vaccinia virus A33R and A36R envelope proteins. J. Virol. **77**:4113–4126.
47. **Wolffe EJ, Isaacs SN, Moss B.** 1993. Deletion of the vaccinia virus B5R gene encoding a 42-kilodalton membrane glycoprotein inhibits extracellular virus envelope formation and dissemination. J. Virol. **67**:4732–4741.
48. **Wolffe EJ, Weisberg AS, Moss B.** 1998. Role for the vaccinia virus A36R outer envelope protein in the formation of virus-tipped actin-containing microvilli and cell-to-cell virus spread. Virology **244**:20–26.
49. **Wolffe EJ, Weisberg AS, Moss B.** 2001. The vaccinia virus A33R protein provides a chaperone function for viral membrane localization and tyrosine phosphorylation of the A36R protein. J. Virol. **75**:303–310.
50. **Zhang WH, Wilcock D, Smith GL.** 2000. Vaccinia virus F12L protein is required for actin tail formation, normal plaque size, and virulence. J. Virol. **74**:11654–11662.